Eur. Phys. J. A **1**, 15–17 (1998)

THE EUROPEAN PHYSICAL JOURNAL A

Short note

Evidence for a neutron skin in ^{20}N

O.V. Bochkarev[1], L.V. Chulkov[1], P. Egelhof[2], H. Geissel[2], M.S. Golovkov[1], H. Irnich[2], Z. Janas[2], H. Keller[2], T. Kobayashi[3], G. Kraus[2], G. Münzenberg[2], F. Nickel[2], A.A. Ogloblin[1], A. Ozawa[3], A. Piechaczek[2], E. Roeckl[2], W. Schwab[2], K. Sümmerer[2], T. Suzuki[3], I. Tanihata[3], K. Yoshida[3]

[1] Kurchatov Institute, RU-123182 Moscow, Russia
[2] Gesellschaft für Schwerionenforschung, D–64291 Darmstadt, Germany
[3] RIKEN, 2-1 Hirosawa, Wako, Saitama 351-01, Japan

Received: 1 October 1997

Abstract. Nuclear interaction and charge-changing cross sections were measured for 950·A MeV ^{20}N, ^{20}O, ^{20}F, ^{20}Ne, ^{20}Na and ^{20}Mg beams incident on a carbon target. The experimental results are compared to other data, in particular to those obtained for stable nuclei. Root mean square nuclear matter radii and upper limits of root mean square proton radii are derived from the experimental data. Evidence is presented for the existence of a neutron skin in ^{20}N.

PACS. 21.10.Ft Charge distribution – 27.30.+t $20 \leq A \leq 38$

The neutron halo phenomenon is one of the most exciting discoveries in nuclear physics of the last decade. Effects ascribed to a neutron halo or a neutron skin[1] have been observed in several nuclei near the neutron dripline [1,2]. These nuclei are of special interest in relation to new properties associated with the neutron excess on the nuclear surface. The difference in the root mean square (r.m.s.) radii of the nuclear matter and proton density distributions (r_m and r_p, respectively) can be used to obtain quantitative evidence of halo or skin effects. The r_m values are usually determined from measurements of high-energy interaction cross section (see, for example, [1] and references therein). The only way to estimate r.m.s. charge radii (r_c) for comparatively short-lived radioactive nuclei is the measurement of optical isotope shifts. However, as was mentioned in [3,4], changes in r_c along an isotopic sequence cannot be unambiguously evaluated for light nuclei owing to the uncertainty of the specific mass shift. A combined analysis of the experimental cross sections for all nuclear interactions (with exclusion of elastic and inelastic scattering) (σ_i) and for those involving changes of the nuclear charge (σ_{cc}) can provide unique information on the difference in proton and neutron densities [5]. We shall use below proton point densities instead of charge densities; the finite size of proton is taken into account by the prescription $r_p^2 = r_c^2 - r_N^2$, with the nucleon r.m.s. radius r_N being equal to 0.8 fm.

In this paper, we present experimental data for σ_i and σ_{cc} for 950·A MeV ^{20}N, ^{20}O, ^{20}F, ^{20}Ne, ^{20}Na and ^{20}Mg beams incident on a carbon target and analysis of these data. The experiment was performed at GSI, Darmstadt, where secondary ^{20}N, ^{20}O, ^{20}F, ^{20}Ne, ^{20}Na and ^{20}Mg beams were produced by a 1050·A MeV primary ^{36}Ar or ^{40}Ar beam impinging on a beryllium target. The $A = 20$ beams of interest were separated from the primary beam and from other reaction products by using the fragment separator FRS. Values of σ_i and σ_{cc} were obtained by means of the transmission method with carbon targets placed at the central focal plane of the FRS (σ_i) and at the final focal plane (σ_{cc}). The second stage of the FRS was used for isotope identification in the measurements of σ_i while only Z-identification was used for the σ_{cc} measurements. The detailed description of the experimental set-up as well as the data on σ_i have been published elsewhere [6].

The σ_{cc} data resulting from this experiment are shown in Fig. 1 in comparison with the σ_i. The σ_i values deviate slightly but irregularly by ±4% from the mean value, reflecting a dependence of r_m on Z. The r_m value of ^{20}Mg is larger than that of its mirror nucleus ^{20}O by ≈ 8%. This phenomenon has been explained as being due to a combined effect of the difference in binding energies of these nuclei and their valence nucleon correlations [7]. Evidence has been found for the existence of a proton skin in ^{20}Mg and a neutron skin in ^{20}N. However, this conclusion was based on r_p values obtained by an extrapolation based on

[1] Qualitatively, the term "neutron skin" describes an *excess* of neutrons at the nuclear surface, whereas "neutron halo" stands for such an excess plus a *tail* of the neutron density distribution

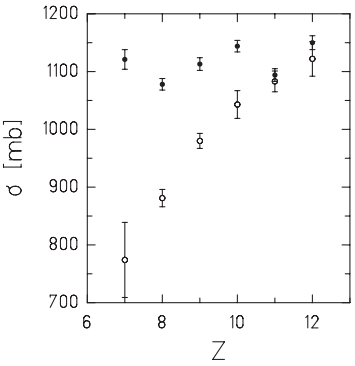

Fig. 1. Interaction (*filled circles*) and charge-changing (*open circles*) cross sections as a function of the atomic number Z for $A = 20$ isobars. The data stem from 950·A MeV reactions on carbon target

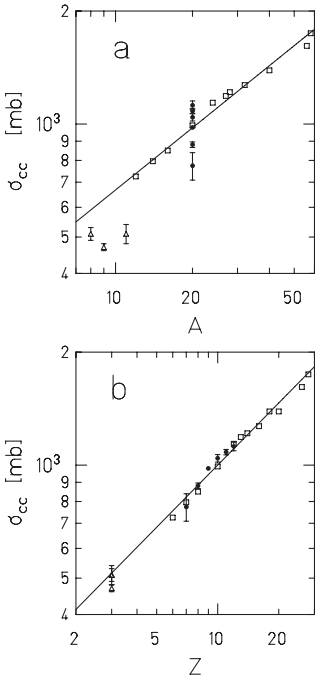

Fig. 2. Doubly-logarithmic plot of the dependence of charge-changing cross sections σ_{cc} on atomic mass A **a** and on atomic number Z **b**. *Open squares* are taken from [8], *open triangles* from [5], and *filled circles* from the present work. The *straight line* in **a** shows the fit of the data by power function of A taken from [8]. The fit of the data by power function of Z is shown in **b** by a *straight line*

experimentally known r_p values of stable isotopes. This was the weak point of our previous analysis in spite of the good agreement of the extrapolated r_p with those predicted by relativistic mean field calculations [6].

As can be seen from Fig. 1, the σ_{cc} values show, contrary to the σ_i behavior, a *strong* dependence on Z, i.e. a decrease by 30 % with Z decreasing from 12 to 7. Within the experimental uncertainties, σ_{cc} is equal to σ_i for the proton-rich nuclei (^{20}Mg and ^{20}Na) whereas it contributes only ≈ 70 % to σ_i in the case of ^{20}N. This effect is similar to that observed for lithium isotopes [5]. The experimental σ_{cc} values are nearly identical for ^{8}Li, ^{9}Li and ^{11}Li, which indicates that the proton distribution stays approximately the same for these isotopes. However, their σ_i values strongly increase with A, which signals variations of the individual r_m values.

For a further discussion of the striking behavior of σ_{cc}, we compare our σ_{cc} data and the results of [5] with those known for stable nuclei [8]. As can be seen from Fig. 2b, σ_{cc} of ^{20}Mg is equal to that of ^{24}Mg (1122 ± 30 mb and 1120 ± 11 mb [8], respectively). Similarly, σ_{cc} of ^{20}N is equal to that of ^{14}N (774 ± 65 mb and 796 ± 8 mb [8], respectively). Following the interpretation given in [5] one may conclude that r_p does not depend strongly on A and remains nearly constant for the isotopes considered. The effect observed in [5] is thus not specific for lithium isotopes including the very neutron-rich, loosely bound ^{11}Li, but reflects the general variation of σ_i and σ_{cc} with A and Z. A further conclusion would be that, for nuclei with given Z, the r_p and thus σ_{cc} values do not show a strong dependence on the neutron number N, while the r.m.s. radii of the neutron density distribution (r_n) and thus σ_i increase more rapidly with increasing N. Similarly, for nuclei with given A the r_p and thus σ_{cc} values decrease rapidly with increasing N. The consequence of these arguments is that σ_{cc} should have a functional dependence on Z but not on A.

However, the data obtained for stable-isotope beams on carbon targets ([8]) show that the A dependence of σ_{cc} can be well described by a power function of A ($\sigma_{cc} \sim A^{0.55\pm0.02)}$) as can be seen from Fig. 2a. On the one hand, σ_{cc} values for drip line nuclei, taken from [5] and the present work and marked in Fig. 2a by triangles and filled circles do not follow such a systematic. On the other hand, all the σ_{cc} values shown in Fig. 2b can be well reproduced by a power function of Z with an exponent 0.55 derived from [8]. The question is whether one can get a more quantitative information beyond this qualitative conclusion.

The r_m values of drip line nuclei have mainly been obtained through the measurements of high-energy interaction cross sections and Glauber model calculations (see [9] and references therein). The Glauber model is based on the assumption that the interactions result from single nucleon-nucleon collisions in the region of overlap between projectile and target (see, e.g., [10]). This model gives the possibility to determine the matter radii by assuming that the nucleus would break up whenever there is an appreciable amount of such an overlap. In the asymptotic energy region, σ_i may, within some limits of accuracy, be approximated by the geometric value: $\sigma_i = \pi(r_m^{target} + r_m^{proj})^2$. When only collisions of projectile protons with target nucleons are taken into account, the resulting cross-section is directly connected with the σ_{cc} value and with the r_p value of the projectile, and thus σ_{cc} values can be used to evaluate r_p.

However, the Glauber mechanism is not the only one which contributes to σ_{cc}. One has to take into account that fragmentation process consists of two steps ([11], for

Table 1. Total interaction cross sections σ_i and charge-changing cross sections σ_{cc} for 950·A MeV $A = 20$ beams incident on a carbon target, together with deduced r.m.s. matter radii, r_m, and upper limits for r.m.s. proton radii, r_p^{max}

Projectile	σ_i [mb]	σ_{cc} [mb]	r_m [fm]	r_p^{max} [fm]
^{20}Mg	1150(12)	1122(30)	2.86(3)	3.18(9)
^{20}Na	1094(11)	1083(18)	2.69(3)	3.14(5)
^{20}Ne	1144(10)	1043(24)	2.84(3)	3.10(7)
^{20}F	1113(11)	980(13)	2.75(3)	2.98(4)
^{20}O	1078(10)	881(15)	2.64(3)	2.72(5)
^{20}N	1121(17)	774(65)	2.77(4)	2.39(20)

example). The fast first step is abrasion, which results in excited fragments and is followed by the slow second step of deexitation (ablation). The deexitation process makes additional contributions to σ_{cc}. This means that the r_p values derived from a fit to the experimental σ_{cc} values by considering only the interactions of projectile protons can thus be interpreted as an upper limit of r_p. We shall show below that this procedure gives the unique possibility to determine the neutron excess in the nuclear surface.

Values for r_m and upper limits for r_p (r_p^{max}) were deduced from our data in the optical limit of the Glauber model. Identical Fermi density distributions with the diffuseness parameter equal to 0.5 fm (see [6] for details) have been used in the both cases. Only the collisions of projectile protons with target nucleons were taken into account in the calculations of r_p^{max}. The results are shown in Tab. .

Except for ^{20}N, all r_p^{max} values are greater than the corresponding r_m data. As was mentioned above, this feature reflects an additional contribution to σ_{cc} from multiple scattering and ablation. For ^{20}N, however, r_p^{max} is smaller than r_m by 0.38 ± 0.20 fm or $15 \pm 8\%$. Correspondingly, the neutron skin, i.e. the difference between r_n and r_p, of ^{20}N is thicker than 0.56 ± 29 fm. This two-standard-deviation effect is in agreement with the results of [6] where the r_p values were obtained by extrapolation from the experimental data for stable isotopes, yielding evidence for the existence of a neutron skin in ^{20}N.

In summary, we conclude that for neutron-rich nuclei the combined analysis of σ_i and σ_{cc} yields an estimate of the difference in the r.m.s. radii of neutron and proton density distributions. The advantage of this method is that the data can be obtained in one and the same experiment which results in a suppression of possible systematical errors. The analysis shows evidence for the existence of a neutron excess at the surface of ^{20}N.

The systematics of the data on σ_{cc} for stable and drip line nuclei reveals that the cross section mainly depends on Z but not on A. This observation may be related to the fact that the difference between r_n and r_p increases monotonically with the difference between neutron and proton numbers or with the difference between the Fermi energies for neutrons and protons. The latter effect can be observed in the proton and neutron separation energies. One should expect that the neutron skin as well as the proton skin is a quite common phenomenon for nuclei close to the neutron or proton drip line, respectively. This conclusion agrees with that drawn on the basis of experimental r_m values for extended series of sodium and magnesium isotopes [12,13] as well as with recent predictions obtained by a relativistic mean-field theory [15], a deformed Hartree-Fock-Bogoliubov model [16] and a spherical Hartree-Fock model [17]. It is interesting to note that the calculations of the r_m and r_p values for ^{20}Mg [15] are in excellent agreement with the experimental data [6].

This work was supported by the Bundesministerium für Bildung und Forschung within framework of Wissenschaftlichtechnische Zusammenarbeitsvereinbarungen under contract number WTZ Bonn RUS 609-96 and by Deutsche Forschungsgemeinschaft (DFG) under contract number 436 RUS 130/127/1.

References

1. Tanihata, I.: J. Phys. G; Nucl. Part. Phys. **22**, 157 (1996)
2. Hansen, P.G., Jensen, A.S. and Jonson, B.: Ann. Rev. Nucl. Part. Sci. **45**, 591 (1995)
3. Huber, G. et al.: Phys. Rev. C **18**, 2342 (1978)
4. Aufmuth, P., Heilig, K., Steudel, A.: Atom. Data and. Nucl. Data Tables, **37**, 455 (1987)
5. Blank, B. et al.: Z. Phys. A **343**, 375 (1992)
6. Chulkov, L.V. et al.: Nucl. Phys. A **603**, 219 (1996)
7. Chulkov, L.V. , Roeckl, E. and Kraus, G. : Z. Phys. A **353**, 351 (1996)
8. Webber, W.R., Kish, J.C. and Schrier, D.A.: Phys. Rev. C **41**, 520 (1990)
9. Ozawa, A. et al.: Nucl. Phys. A **608**, 63 (1996)
10. Karol, P.J.: Phys. Rev. C **11**, 1203 (1975)
11. Gaimard, J.-J. and Schmidt, K.-H.: Nucl. Phys. A **531**, 700 (1991)
12. Suzuki, T. et al.: Phys. Rev. Lett. **75**, 3241 (1995)
13. Suzuki, T. et al.: Nucl. Phys. A **616**, 286c (1997)
14. Brohm, T. et al.: Nucl. Phys. A **550**, 540 (1992)
15. Ren, Z. et al.: Phys. Lett. B **380**, 241 (1996)
16. Grümmer, F. et al.: Phys. Lett. B **387**, 673 (1996)
17. Brown, B.A. and Richter, W.A.: Phys. Rev. C **54**, 673 (1996)